

# Simplified Techniques to Study Components of Solar Radiation Under Haze and Clouds<sup>1</sup>

MARVIN L. WESELY

*Radiological and Environmental Research Division, Argonne National Laboratory, Argonne, IL 60439*

(Manuscript received 21 July 1980, in final form 3 November 1981)

## ABSTRACT

Estimates of the global ( $G$ ), diffuse ( $D$ ) and direct-beam ( $I$ ) irradiances at the surface of the earth can be obtained with a single instrument, the "dial" radiometer. The dial assembly intermittently shades a solid-state sensor on a continual automatic basis. This is a very simple instrument that does not require mechanical adjustments of the shade. When corrections for imperfect cosine response and excessive shading of sky radiation are performed, measurements averaged over 1 h should be accurate well within  $\pm 5\%$ . Estimates of atmospheric turbidity or haziness can be expressed as an extinction coefficient, computed for  $I$  in reference to that obtained under cloudless clean skies for the same solar zenith angle. The uneven spectral response of silicon-cell and PAR (photosynthetically active radiation) sensors should be considered when comparing estimates of  $G$ ,  $D$  or  $I$  to measurements of these components by a wide-band sensor. Linear relationships seem adequate for a variety of cloud conditions. This allows the use of a single dial silicon-cell radiometer, for example, to estimate quite accurately the values of  $G$ ,  $D$  and  $I$  that would be seen by wide-band or PAR radiometers. An alternative, but less exact, means of obtaining estimates of hourly averages of  $D$  and  $I$  is to measure only  $G$  and use the ratio of  $G$  to that which would be obtained under clean, cloudless conditions as the sole determining factor.

## 1. Introduction

Global ( $G$ ) solar irradiance received at the surface of the earth can be divided into two components, direct-beam and diffuse. More clouds and haze in the atmosphere usually increases the diffuse and decreases the direct-beam radiation, except in the case of overcast skies when the mean direct-beam component falls to nearly zero and the mean diffuse radiation decreases as the optical depth of the clouds increases. Measurement or knowledge of such variations in diffuse ( $D$ ) and direct-beam ( $I$  for incident) radiation, in addition to  $G$ , is needed in order to study the effects of air pollution on climate, the responses of biological systems to solar radiation, the performance of man-made solar energy collectors, and the design of buildings for energy conservation. To measure solar irradiance, a pyranometer can be used for  $G$ , a pyrheliometer for  $I$ , and a pyranometer with a shade ring or occulting disk for  $D$  (e.g., see Coulson, 1975). Usually, determination of all three components requires at least two of the instruments; one of the components, usually  $D$  or  $I$ , can be found by difference. In this paper, the use of only one instrument, the dial radiometer, to estimate all three irradiances is explored. Silicon-cell and PAR (photosynthetically active radiation) sensors are used in the dial assembly and compared to standard solar sen-

sors. Also, a method is developed to estimate  $D$  and  $I$  when only  $G$  is measured.

All data were obtained during summer over a green surface, mostly at Argonne National Laboratory. Since no attempt is made to determine explicitly the effects of absorption and scattering by atmospheric water vapor, some of the results would be systematically different during cooler seasons when precipitable water vapor is less. For example, the component  $I$  under cloudless skies would increase as precipitable water decreases, for the same solar zenith angle. The surface albedo would also be different during other seasons or with other surfaces, and this might have a considerable effect on the behavior of  $D$ . Nevertheless, the theoretical aspects of procedures used here to derive relationships between  $G$ ,  $D$  and  $I$  should be applicable under such altered conditions.

## 2. The dial assembly

The radiation sensor used to measure solar radiation must respond quickly so that the sensing element can be rapidly shaded and unshaded. For this purpose, a "silicon-cell pyranometer" commercially available from LAMBDA Instruments Corporation<sup>2</sup> is suitable. Such instruments respond fully in less

<sup>1</sup> Work performed under the auspices of the U.S. Department of Energy.

<sup>2</sup> This does not connote approval or recommendation of the product by Argonne National Laboratory or sponsors, to the exclusion of other products that may be suitable.



FIG. 1. The dial assembly with a cosine-corrected silicon sensor in place beneath the occulting strip. The actual sensing area to be shaded is the white disk at the center of the radiometer head. In use, the device is leveled and mounted so that the occulting arm can pass under the box.

than 0.001 s, are partially cosine-corrected by a Scripps head (Kerr *et al.*, 1967), and are small (outside dimensions  $\sim 2.5$  cm). Calibration drifts of the LAMBDA sensor are small, found to be less than  $\pm 2\%$  after five years of operation at Argonne. For PAR detection, a "quantum" sensor replaces the silicon device and is identical (as made by LAMBDA)

except for optical filtering added in order to obtain the desired spectral response.

The radiation sensor is placed on a small leveling platform and situated as shown in Fig. 1. The total assembly is called the "dial" radiometer both because the rotating shade resembles the face of a dial with a revolving arm and because the device is used

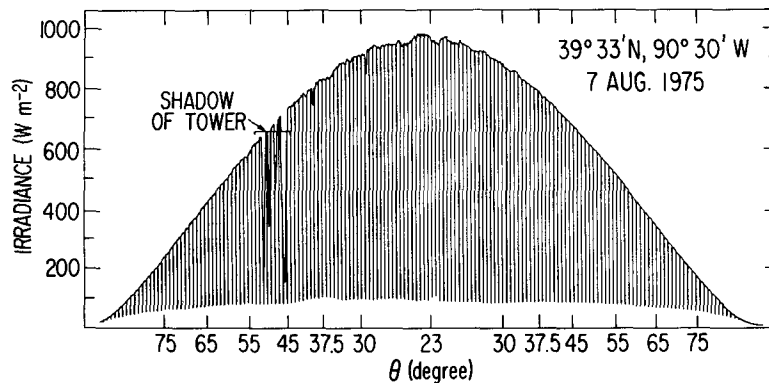


FIG. 2. An example of solar radiation measured with the dial silicon-cell radiometer during an exceptionally cloudless, clear day in southeastern Illinois. The abscissa is in units of zenith angle but actually bears a linear relationship to time of day, with morning on the right-hand side.

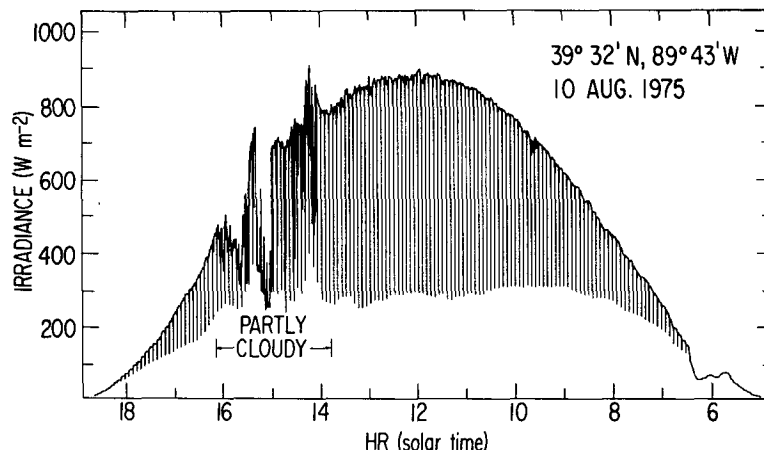


FIG. 3. An example of the output of the dial silicon-cell radiometer during a very hazy day in central Illinois.

to measure “*D*-and-*I-AL*” quantities. The chassis box shown in Fig. 1 contains a motor to turn the shaft and the attached shading strip. The small synchronous motor, with speeds of 0.20 or 0.25 rpm, allows shading to occur approximately every 4 or 5 min. To use this device, one levels it and positions it such that the shaft is exposed on the south side (north side in the Southern Hemisphere). Maintenance consists of cleaning the sensing area and checking the level. No shade adjustments are needed, provided the strip is sufficiently long to shade the sensing element for all the solar azimuth and zenith angles of interest.

A downward spike in the output of the dial radiometer occurs during each shading, with magnitude corresponding to the direct-beam irradiance. Examples of the output of the sensor are shown in Figs. 2-4. Of course, when the sensor is not shaded, global irradiance is measured, and the distance from the minima of the spikes to the zero level corresponds to the diffuse irradiance. Thus, *I*, *G* and *D* are all measured by a single instrument.

In the present configuration, the occulting strip is  $\sim 0.9$  cm wide and  $\sim 6.0$  cm away from the 0.8 cm

diameter sensing element. With the shade sweeping a circle 11 cm in radius every 4 or 5 min, the sensor is partially shaded for at least 7 s, shaded but with minor penumbra for  $\sim 0.7$  s, and in the umbra for slightly more than 0.1 s. This is sufficient time for modern strip-chart recorders to respond and display the minima with negligible error; with electronics designed to detect the minimum value, the speed of rotation could be increased considerably.

### 3. Limitations of the dial radiometer

Several unique aspects of the dial radiometer must be considered in order to compare this method of obtaining *D* and *I* with other methods. First, a fairly large portion of the sky is masked near the sun, with an angle subtended of  $\tan^{-1}(b/r) \approx 10^\circ$  where *r* is the distance from the sensor to the shading arm and *b* the diameter of the shading element. This angle is about twice that normally recommended (e.g., Coulson, 1975). Diffuse irradiance measured with the dial radiometer is therefore slightly underestimated and the direct-beam slightly overestimated, as compared to more ideal arrangements. The mag-

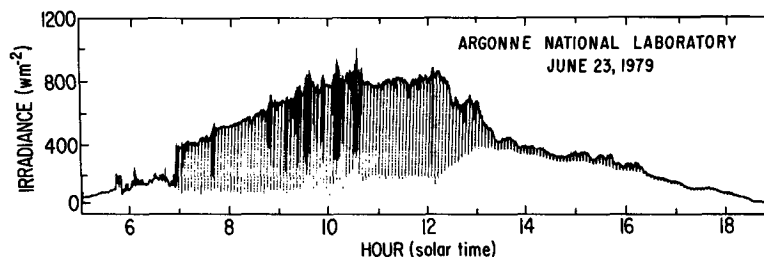


FIG. 4. Measurements of solar radiation by the dial silicon-cell radiometer under varying cloud conditions. Cumulus clouds were present between 0845 and 1030 LT, cirrus were predominant from 1030 to 1215 LT, and altostratus provided a nearly overcast sky from 1330 LT to sunset.

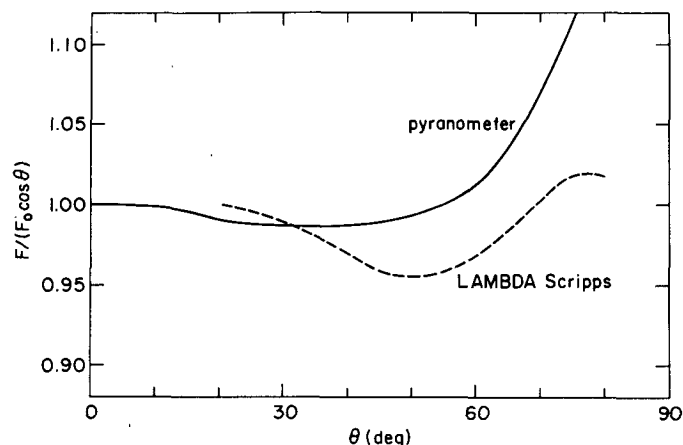


FIG. 5. Relative cosine responses of the sensors used in the present study.

nitudes of the errors undoubtedly depend on the amount and characteristics of the airborne particulate material and cloud present. In this paper, dial data are compared with measurements obtained in part from a pyranometer shaded with a small disk (Wesely and Lipschutz, 1976a) that likewise subtends an angle of  $\sim 10^\circ$ , making comparisons at least self-consistent. Experiments conducted by employing various sizes of occulting disks with the pyranometer during very hazy conditions indicate that variations in  $D$  are  $<3\%$  as the angle subtended changes from about  $5$  to  $15^\circ$ . Although these errors are small, they are systematic and should be kept in mind when comparing results to other experimental efforts.

Perhaps a more serious error is caused by the shading arm covering a substantial portion of the sky in addition to that within  $10^\circ$  of the sun, resulting in underestimates of the diffuse radiation. An analysis based on calculation of view factors can be performed (e.g., Bird *et al.*, 1960) to show that the diffuse radiation from isotropic scattering from a uniformly illuminated sky is reduced by the fraction  $1.5b(\pi r)^{-1} \cos \eta$ , where  $\eta$  is the angle the shade has rotated around the shaft from zenith to the position that causes a shadow to be cast on the sensing area. This fraction can be compared to the maximum value of  $2b(\pi r)^{-1}$  found by Drummond (1956a) for a narrow shading strip that extends across the entire daily path of the sun, rather than the present case of a strip across  $120^\circ$  of the hemisphere. Hence, the diffuse radiation measured with the dial radiometer should be multiplied at least by the factor  $\gamma = (1 + 0.086 \cos \eta)$ , given  $b = 0.9$  cm and  $r = 5.0$  cm. An analysis in geometry shows that  $\cos \eta$  is given as

$$\cos \eta = \cos \theta (\cos^2 \theta + \sin^2 \alpha \sin^2 \theta)^{-1/2}, \quad (1)$$

where the solar zenith angle  $\theta$  and the azimuth angle  $\alpha$  can be calculated directly if latitude, declination angle and hour angle are known (e.g., Coulson, 1975; Paltridge and Platt, 1976).

As shown by Drummond (1956a), a correct factor such as  $\gamma$  is usually a slight underestimate because scattering is partially anisotropic in all cases except when skies are heavily overcast. For a fixed shadow band extending across the entire hemisphere and with a value of  $b/r$  similar to that for the dial radiometer, Drummond (1956b) finds that the corresponding  $\gamma$  should be increased to  $(\gamma + 0.04)$  for clear skies and to  $(\gamma + 0.02)$  for partly cloudy skies (both regardless of  $\theta$  or  $\eta$ ). Also, from the discussions by Drummond, it appears that  $(\gamma + 0.07)$  should be used for very hazy conditions (and skies with thin cirrus, presumably). The correction factors for the dial radiometer should be similar but must be adjusted for less sky coverage by the shading element. The likely correction factors are  $\gamma$  for heavily overcast skies,  $(\gamma + 0.015)$  for partly cloudy skies (not thin cirrus),  $(\gamma + 0.03)$  for clear fairly-clean skies, and  $(\gamma + 0.05)$  for hazy conditions (or skies with thin cirrus). All the data in this paper, with a few exceptions that are noted, include the factor  $(1 + 0.1 \cos \eta)$ , and  $I$  is adjusted accordingly. Thus,  $D$  will be slightly underestimated and  $I$  slightly overestimated by the dial radiometer a substantial portion of the time. Further, since the axis of shade rotation is slightly off center,  $b/r$  is slightly smaller when  $\eta$  is larger, and this might reduce the relative errors slightly when the sun is near the horizon.

The solar sensors used in this study do not have perfect cosine response. As shown by Secret and Dirmhirm (1979), cosine response errors as well as effects due to the shading of sky radiation should be considered when  $I$  is calculated as the difference between  $G$  and  $D$ . Fig. 5 shows the cosine responses, measured in the laboratory, of the instruments used in this study. The cosine response factor is given as the ratio of  $F$  to  $F_0 \cos \theta$ , where  $F$  is the sensor response to irradiance  $F_0$  found when the angle of rotation  $\theta$  is zero. All the LAMBDA devices used have approximately the same cosine response and have

factors that agree fairly well with the manufacturer's estimates. The cosine response factor for the pyranometer used to measure  $G$  is slightly less than that found for newer devices of the same type, probably because the sensor had been repaired with small amounts of glue where the glass dome is attached to the metal base. A second-degree polynomial can be found to describe adequately the cosine response factor for the pyranometer, and a third-degree polynomial fit is adequate for the LAMBDA instruments. The estimates of  $I$  obtained in this study were all adjusted, with a few exceptions noted, to account for cosine response errors.

It can be seen in Fig. 5 that the cosine response correction for  $I$  from both sensors is less than 5% for  $\theta \leq 65^\circ$ . With the dial radiometer, the effects of errors associated with the shade arm on raw estimates of  $D$  results in overestimates of  $I$ , counter to the effects of imperfect cosine response. Thus, at moderate to small zenith angles, raw uncorrected values of  $I$  from the sensors used in this study should be accurate well within  $\pm 5\%$ , if there are no other sources of error.

Another difference between the photocells and the pyranometer is that the silicon device and the PAR sensors have uneven spectral response to solar radiation, in contrast to the wide-band response of ideal pyranometers. It is well known that the silicon cell responds most strongly to radiation of wavelengths near  $0.85 \mu\text{m}$ , not very well to blue, and has effectively no response to radiation of wavelengths  $> 1.2 \mu\text{m}$ . Thus, the silicon cell detects the blue sky radiation poorly and should not be affected by the rather strong absorption of radiation by water vapor at wavelengths  $> 1.0 \mu\text{m}$ . Since the PAR sensor is tailored to respond to radiation of wavelength  $0.4\text{--}0.7 \mu\text{m}$ , diffuse radiation during cloudless conditions evokes a rather strong response; absorption of radiation by water vapor and carbon dioxide has very little influence in comparison to the effect on a true pyranometer.

Finally, a practical limitation to the use of the dial radiometer deals with data reduction. Direct electronic integration of the signals leading to the displays shown in Figs. 2–4 yields 3–5% underestimates of global solar irradiation, due to partial shading of the sensor from both diffuse and direct radiation. To obtain better estimates of  $G$ , one should integrate portions of the signals corresponding only to the 2 min or so when the shade is in the lower hemisphere, as was done for the data in this paper. Also, locating the minima to determine values of  $D$  during partly cloudy conditions can be difficult. At Argonne, we have found that  $\sim 1$  h of work is necessary to obtain accurate values of  $G$  and  $D$  from strip-chart records for a period of one week. However, the speed of such data reduction depends greatly on the amount of prior operator experience and on the degree of au-

tomation used to record discrete values as the charts are traced manually. In our case, the values were read and recorded manually. Clearly, the costs of manual data reduction or of developing proper electronics should be kept in mind when considering acquisition and deployment of the dial radiometer as an alternative to more expensive direct and global radiation sensors.

#### 4. Cloudless, clean skies

Cloudless, clean skies are considered first in order to derive the values of diffuse and direct irradiance,  $D_0$  and  $I_0$ , respectively, that are not affected by cloud or haze. When these are used as normalizing factors for  $D$  and  $I$ , simple parameterization schemes can be developed to describe the effects of clouds and haze, as will be evident later. Examination of several years of data has led to the observation that usually 3–6 days of exceptionally cloudless and clean conditions can be found every year from about mid-April to mid-September in Illinois. The irradiances from a dial silicon-cell radiometer for such a day are shown in Fig. 2. An example of values of  $D_0$  and  $I_0$  found with the pyranometers used in the present study but not corrected for shading errors or imperfect cosine response is given by Wesely and Lipschutz (1976a) in their Figs. 3 and 4. Thus, estimates of  $D_0$ ,  $I_0$  and  $G_0 = D_0 + I_0$  can be found as a function of solar zenith angle  $\theta$ , which is readily calculated from knowledge of true solar time, latitude and declination angle (e.g., see Paltridge and Platt, 1976).

Use of this technique to obtain  $I_0$  and  $D_0$  has the advantage that they are determined quite easily and that calculations based on altitude, atmospheric water vapor content, atmospheric ozone concentrations or surface albedo are not necessary. The approach used here, however, restricts use of the present estimates of  $D_0$  and  $I_0$  to locations at elevations near 200 m above mean sea level in the midlatitudes over green surfaces, and to moderately humid environments where the total precipitable water is  $\sim 2$  cm.

Another consideration is that the solar "constant" varies during the year because the distance from the sun to the earth in its elliptic orbit changes slightly. All values of irradiance in this paper have been scaled by the square of the ratio of the sun-earth distance as given by Paltridge and Platt (1976), thus eliminating most of the effects of this natural variation.

Table 1 gives the mean values of  $D_0$  and  $I_0$  found for selected zenith angles. The calibration for the silicon cell is that given by the manufacturer and undoubtedly is meant to apply without qualification only to  $G$  obtained during clean, cloudless conditions and when solar zenith angles are rather small. Thus, while  $G$  at such times should be the same for the pyranometer and the silicon cell within  $\pm 2\%$ , there

TABLE 1. Summary of measurements taken during the summer of 1976 and 1977 at Argonne under cloudless skies. Standard errors are shown for the slopes and  $b$  is the intercept resulting from least-squares analysis. For  $D_0$  and  $I_0$ , the standard errors are typically 3 and 5  $W m^{-2}$ , respectively.

$\theta$ (deg)	Wide-band solar				Solar from Si			
	$D_0$ ( $W m^{-2}$ )	$I_0$ ( $W m^{-2}$ )	$dD/dI$	$b$ ( $W m^{-2}$ )	$D_0$ ( $W m^{-2}$ )	$I_0$ ( $W m^{-2}$ )	$dD/dI$	$b$ ( $W m^{-2}$ )
30	73	796	$-0.612 \pm 0.042$	565	52	823	$-0.640 \pm 0.040$	578
37.5	72	714	$-0.668 \pm 0.030$	553	52	752	$-0.642 \pm 0.030$	533
45	70	630	$-0.611 \pm 0.022$	457	49	660	$-0.622 \pm 0.022$	461
55	61	499	$-0.585 \pm 0.023$	352	45	516	$-0.620 \pm 0.027$	362
65	56	328	$-0.590 \pm 0.025$	243	39	344	$-0.624 \pm 0.025$	250
75	41	161	$-0.545 \pm 0.029$	127	34	175	$-0.577 \pm 0.035$	134

is no assurance that  $D$  and  $I$  individually from the silicon photocell should be so accurate. Table 1 shows that  $D$  is underestimated and  $I$  is overestimated by the silicon cell. This is expected because, as stated above, the silicon photocell has the disadvantage of responding to red and far red radiation much more strongly than the blue light of diffuse radiation from cloudless skies.

As shown by Wesely and Lipschutz (1976a), certain forms of empirical functions should be adequate for describing  $D_0$  and  $I_0$ . These are provided in Table 2, with the numerical values found as a result of statistical least-squares analyses; the values obtained correspond to those which could be found by use of a Langley plot. Comparison of the exponential values in the expressions for  $I_0$  given in Table 2 shows that as the sensor shifts in maximum sensitivity from red to blue (Si  $\rightarrow$  solar  $\rightarrow$  PAR), greater losses of the direct-beam component are detected as the optical air mass increases. This results simply because the Rayleigh scattering in cloudless skies is more efficient for blue light. For the same reason, sensors more sensitive to blue light see a greater proportion of  $G$  as diffuse radiation, as is evident in Tables 1 and 2.

### 5. Hazy, cloudless skies

The dial silicon-cell radiometer was first conceived as a simple means to obtain estimates of atmospheric turbidity, and has been used for that purpose in a network of sites in the northeastern United States during 1977 and 1978 (Shannon *et al.*, 1978). The interpretation of results from such a sensor is discussed below.

Fig. 6 shows data on  $D$  vs  $I$  collected during the summers of 1976 and 1977 at Argonne, both from the dial silicon-cell radiometer and the pyranometer system (one pyranometer shaded with a small disk and one unshaded). The slopes of  $D$  vs  $I$  have an important interpretation with regard to the effective albedo of the earth; this has already been discussed by Wesely and Lipschutz (1976a). Table 1 gives numerical values of the slopes and their standard errors found by linear least-squares analysis. The slopes are not significantly different for the two sensors. Since the silicon cell is mostly responsive to red and far-red radiation while the pyranometer has uniform spectral response, the approximate agreement in values of slopes indicates that the effects of absorption and scattering of solar radiation by haze does not seem to be strongly dependent on the wavelength of solar radiation, for the aerosols encountered.

For these same data, the aerosol extinction coefficient is calculated as

$$\tau_a = -m^{-1} \ln(I/I_0), \quad (2)$$

where  $m = \sec\theta$  is the optical air mass number. Fig. 7 shows the results. There is considerable scatter in the data at  $\theta = 75^\circ$ , probably because small errors in the determination of true solar time result in rather large errors in the estimates of  $\tau_a$ . For  $\theta \leq 65^\circ$ ,  $\tau_a$  from the pyranometers is found by least-squares analysis to be equal to the dial  $\tau_a$  multiplied by  $1.019 \pm 0.15$  plus an offset of  $0.021 \pm 0.003$ . An  $R^2$  value of 0.96 is found for the 194 observations. The deviation of this result from the more desired case of the proportionality factor being unity and the offset

TABLE 2. Empirical functions to describe  $D_0$  and  $I_0$  for fine summer conditions at Argonne. The quantity  $m = \sec\theta$  is the optical air mass.

	$D_0$	$I_0$
Solar ( $W m^{-2}$ )	$36 + 54m^{-1} \exp(-0.145m)$	$1095m^{-1} \exp(-0.145m)$
Solar from Si ( $W m^{-2}$ )	$29 + 32m^{-1} \exp(-0.130m)$	$1125m^{-1} \exp(-0.130m)$
PAR ( $\mu E m^{-2} s^{-1}$ )	$150 + 70m^{-1} \exp(-0.256m)$	$2870m^{-1} \exp(-0.256m)$

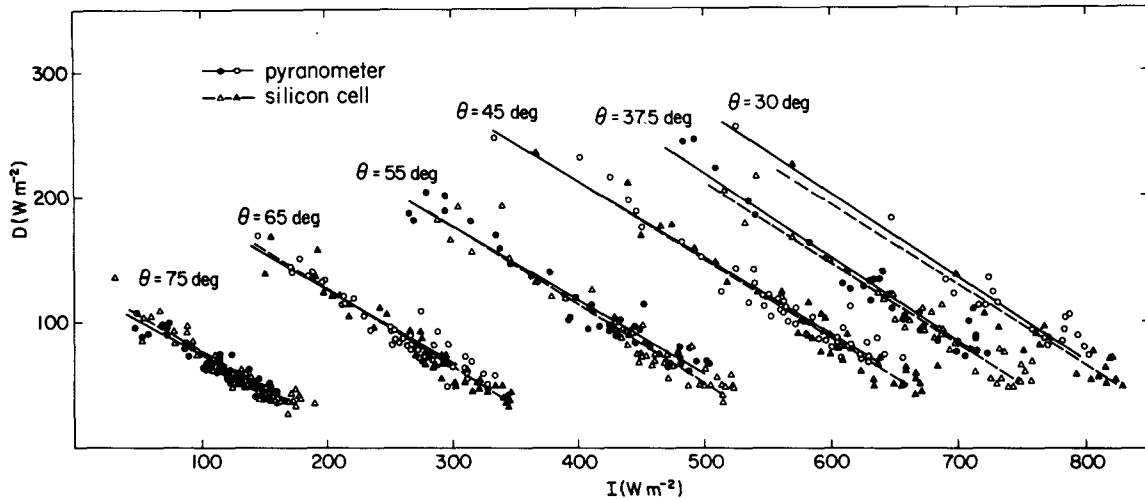


FIG. 6.  $D$  versus  $I$  for the pyranometer system and the dial silicon-cell radiometer operated simultaneously under cloudless skies during summer at Argonne. Expressions for the straight lines are given in Table 1. Open as well as closed symbols are used only to help distinguish data for different values of  $\theta$ .

being zero might be caused by inadequacies in the corrections for excessive shading by the dial radiometer, by inaccuracies in the estimates of  $I_0$ , by true geophysical processes, or, most likely, by a combination of these considerations. It is noteworthy that nearly identical results on a comparison of  $\tau_a$ 's are also found (Wesely *et al.*, 1978) if the estimates of  $I_0$  and  $I$  are derived without shade or cosine-response corrections (the effects of solar "constant" variations are routinely accounted for).

It is very likely that the scatter of the data in Figs. 6 and 7 is mainly due to difficulties caused by inaccuracies in obtaining good readings of sensor outputs and in precisely determining true solar time, plus perhaps other problems such as keeping sensors clean and leveled. For the purpose of estimating  $\tau_a$ , the statistics generated by analysis of the data in Fig. 7 indicate that most single readings of dial  $\tau_a$  are accurate to within  $\pm 30\%$ , for  $\theta \leq 65^\circ$ .

### 6. Cloudy skies

It is well known that the effects of clouds on solar radiation components are difficult to parameterize for the rather short time periods of  $\sim 1$  h, because of the great variations in the optical density of clouds and their frequent nonuniform distribution across the sky, among other reasons. Even various methods for estimating total cloud cover over long periods of time have systematic differences (Hoyt, 1977). Usually, estimates of global radiation based on cloud cover and knowledge of extraterrestrial radiation are highly accurate only if averaging periods of at least several days are employed (Davies, 1979). The separation of global irradiance into diffuse and direct compo-

ponents is more difficult to predict, and empirical relationships for daily and monthly averages are often employed, largely derived from studies such as those by Liu and Jordan (1960) and Stanhill (1966). The universality of such relationships, however, can be questioned (e.g., Ruth and Chant, 1976). In this section, the utility of the silicon-cell and PAR dial radiometers for measurements of hourly averages of components of solar radiation under cloudy skies is explored. The technique is sufficiently simple to be considered an alternative to the use of sunshine re-

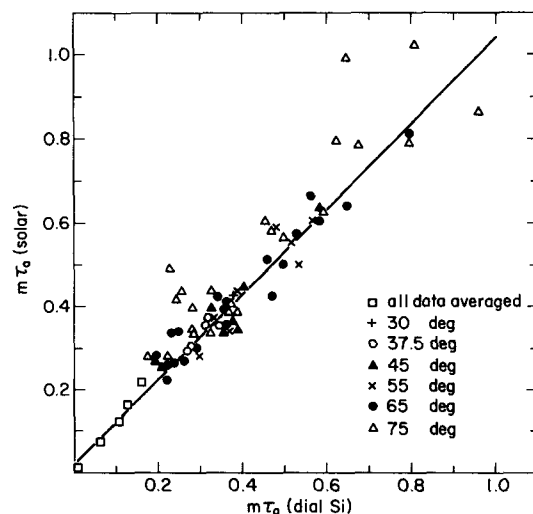


FIG. 7. Determinations of  $m\tau_a$  (where  $m$  is the optical air mass) obtained with the pyranometer system compared to simultaneous estimates obtained with the dial silicon-cell radiometer, for the solar zenith angles indicated. The straight line results from a linear regression analysis.

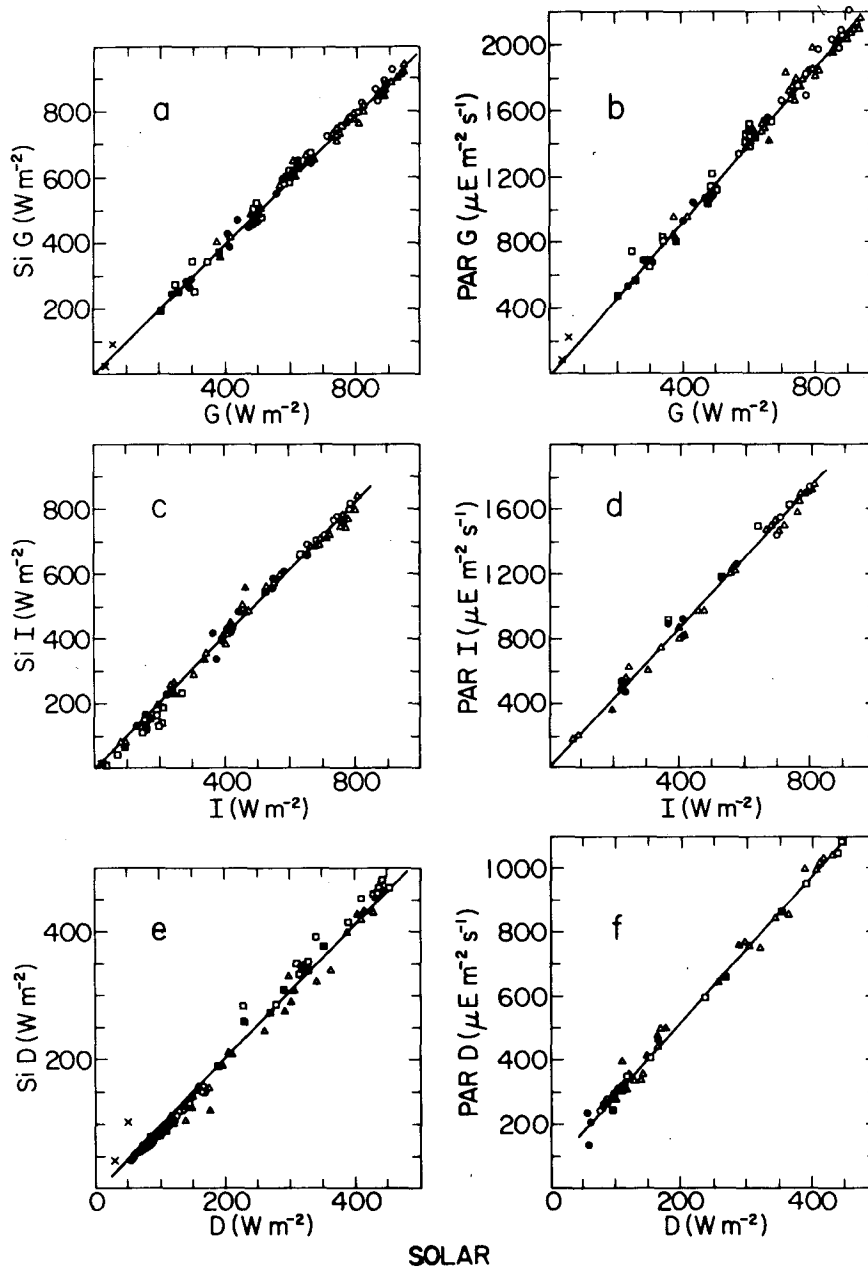


FIG. 8. Hourly averages of solar components measured with dial radiometers versus similar measurements obtained with the pyranometer system, at Argonne during June and July, 1979. The symbols correspond to different types of clouds: circles for cloudless skies, triangles for high-level clouds, squares for middle- and lower-level clouds, and X's for heavily overcast conditions. Open symbols are for data obtained when the solar zenith angle was greater than about  $45^\circ$ , closed for less than  $45^\circ$ .

corders to estimate solar radiation components (e.g., Schulte, 1976).

Fig. 8 shows the results of a study comparing the dial estimates of hourly averages of global, direct and diffuse irradiances with those obtained with Eppley black-and-white pyranometers, the same system used for comparisons earlier in this paper and de-

scribed more fully elsewhere (Wesely and Lipschutz, 1976a,b). Data were collected for several days during the summer at Argonne National Laboratory, under a variety of cloud conditions and solar zenith angles. With the methods described earlier, all data were adjusted to minimize the effects of cosine-response errors, shading of sky radiation by the dial radi-



TABLE 3. Summary of regression analyses on data shown in Fig. 8 relating the solar components measured with silicon-cell and PAR sensors in dial assemblies to data from two wide-band pyranometers, one of which is shaded with an occulting disk. Only data for zenith angles  $< 75^\circ$  are used. The  $R^2$  values are all greater than 0.98.

a) Si $G = 1.00G$	c) Si $I = 1.02I$	e) Si $D = -18 + 1.09D$
b) PAR $G = 2.30G$	d) PAR $I = 2.18I$	f) PAR $D = 55 + 2.31D$

ometers, and the well-known yearly trends in the solar "constant."

Figs. 8a and 8b show a comparison of hourly averages of global irradiances. The calibration for the silicon cell seems to hold up very well under varying cloud conditions and solar zenith angles; no alteration to the calibration constant obtained under clear skies and small zenith angles is needed. Kerr *et al.*, (1967) found similar results for daily averages obtained with such a silicon-cell device. This implies that the spectral content of global radiation is not greatly changed by clouds. The effects of clouds on global PAR is likewise very straightforward and a linear relationship is quite adequate to relate  $G$  from the PAR sensor to that from the pyranometer. Table 3 summarizes the expressions, derived from linear regressions, for the straight lines drawn in Fig. 8.

Figs. 8c-8f indicate that linear expressions are also quite adequate to relate the direct and diffuse components obtained by the three sensors. As expected, the silicon cell is more sensitive to the direct-beam component than to diffuse radiation, which contains a substantial amount of blue light. For very cloudy conditions, the silicon cell overestimates the diffuse radiation by a fraction nearly the same as that for

the direct beam, probably because the blue portion of the solar spectrum is not very important for diffuse radiation under clouds (Federer and Tanner, 1966). In an inverse manner, the PAR radiometer is slightly less sensitive to direct than to global radiation and is more sensitive to diffuse radiation, under mostly clear skies. In summary, from the evidence gathered here and the expressions given by Table 3, it appears that hourly averages of the individual components of radiation detected by the silicon cell, the PAR sensor, and the pyranometer under cloudy conditions are related very simply by linear expressions, accurate to within  $\pm 5\%$  for most single estimates. Thus, a single dial radiometer can be used to estimate all of these components.

A final consideration is whether the diffuse and direct components can be estimated from a measurement of global radiation alone. Hourly averages under cloudy skies are again considered. Such attempts are not uncommon (e.g., Bruno, 1978), but here we consider formulations based on selected physical arguments, with the result that some advantages are obtained. To begin, the wide-band pyranometer values from Fig. 8 are replotted as shown in Figs. 9 and 10. The general shape of the curves formed by the data does not appear to be dependent on solar zenith angle, and also is not affected by cloud type (this latter observation is not illustrated in Figs. 9 and 10 in order to preserve clarity). The greater scatter at large solar zenith angles probably results from the effects of uneven cloud distribution in the sky. Long periods of time elapse at large zenith angles either with the effects of few or isolated clouds blocking the direct beam or with a large amount of

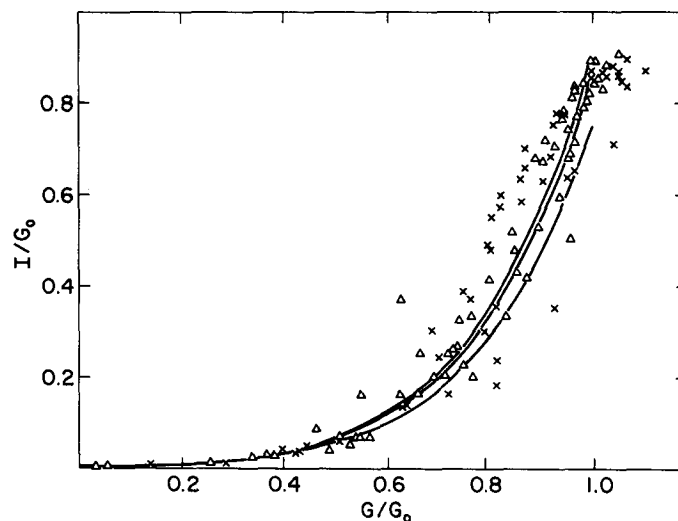


FIG. 9. Hourly averages of  $I$  versus  $G$  measured with the wide-band pyranometer system, for  $\theta < 75^\circ$ . The normalizing factor  $G_0$  is a computed hourly average. Triangles refer to cases with  $\theta < 45^\circ$ , X's to  $\theta > 45^\circ$ . The solid lines correspond to (3) with values of  $20^\circ$ ,  $55^\circ$  and  $75^\circ$  for  $\theta$ , from top to bottom.

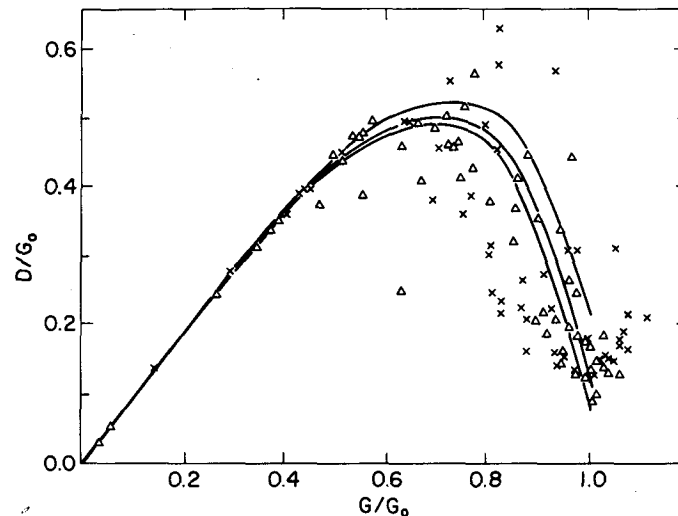


FIG. 10.  $D$  versus  $G$  from the same observations as cited for Fig. 9. The solid lines correspond to (4) with values of  $75^\circ$ ,  $55^\circ$  and  $20^\circ$  for  $\theta$ , from top to bottom.

cloud overhead increasing diffuse radiation but not interfering with the direct beam.

The shape of the curves in Figs. 9 and 10 are strongly affected by the normalizing factor chosen. The use of  $G_0$  as the factor has the advantage that data obtained with varying solar zenith angles  $\theta$  can be plotted to form the same curve, ideally. Extraterrestrial radiation performs a similar function (Bruno, 1978), but does not have some of the built-in variation with  $\theta$  that  $G_0$  does for cloudless skies. Use of  $G_0$  allows better correlation of the normalizing factor with the variations of  $D$  and  $I$  with  $\theta$ , especially for cloudless or partly cloudy skies.

The form of the data in Fig. 9 suggests something akin to an exponential relationship between  $I/G_0$  and  $G/G_0$ . Ideally when  $G/G_0$  is unity,  $I/G_0$  should be equal to  $I_0/G_0$ . A statistical analysis finds that the expression

$$I/G_0 = I_0 G_0^{-1} \exp[5(G/G_0 - 1)], \quad (3)$$

provides an excellent fit with an  $R^2$  value of 0.96 for the logarithmic quantities. This implies that the optical thickness of the clouds is on the average given by  $(1 - G/G_0)$ . The reason for this is not entirely evident, but undoubtedly is related to the fact that a significant fraction of the direct-beam irradiance attenuated by clouds (or haze) is regained as diffuse radiation, a component of  $G$ .

If we assume that (3) is valid, then  $D$  can be expressed as  $G - I$ , or

$$D/G_0 = G/G_0 - I_0 G_0^{-1} \exp[5(G/G_0 - 1)]. \quad (4)$$

As shown in Fig. 10, this expression provides a good fit to the data.

## 7. Conclusions

The dial radiometer provides a simple means to measure the components of solar radiation. The device is easy to install and provides an output that is readily interpreted. To date, strip-chart recorders have been used to record the output; development of more sophisticated electronic devices for data collection and analysis would reduce the task of data reduction. Commercially available solid-state sensors are quite adequate for use in the dial assembly, but some care must be taken in interpreting the measured diffuse irradiance if the spectral response of the device is not uniform.

A vertically-integrated estimate of atmospheric turbidity, expressed as an extinction coefficient, can be obtained with the dial silicon-cell assembly to within an accuracy of  $\pm 30\%$  for single readings, when solar zenith angles are  $65^\circ$  or less. Of course; more precise estimates are obtained with repeated sampling. If accuracies  $> \pm 5\%$  are desired, corrections for imperfect cosine response and excessive shading of sky radiation by the dial assembly should be performed. Averaged results should compare within  $\pm 2\%$  of those obtained with wide-band pyranometry when the same computational procedures are employed.

Clouds greatly modify the nature of solar radiation reaching the surface of the earth. Due to nonuniform spectral response, silicon cells underestimate the diffuse and overestimate the direct-beam irradiance under clear skies, but become more accurate as cloudiness increases. The silicon devices measure global irradiance (hourly averages) very well under nearly all conditions. Because of spectral weighting,

PAR sensors provide more relative output for diffuse radiation from clear portions of the sky and less for direct-beam radiation. The equations given in Table 3 provide a means to relate quite accurately the hourly averages of  $G$ ,  $I$  or  $D$  from one of the three types of sensors (wide-band, silicon-cell, or PAR) to that from another type. An alternative to direct measurements of  $I$  and  $D$  is to measure only  $G$  with a silicon photocell or a standard wide-band pyranometer. Employing (3) and (4) and Table 3 then allows rough estimation of hourly averages of the component desired.

*Acknowledgments.* This work was supported by the U.S. Department of Energy through the Office of Health and Environmental Research, for the MAP3S program at first and later as part of climate-related research. The data were collected with the assistance of Mr. Frank Kulhanek. Much of the data reduction and preliminary analysis was performed by Mr. William W. Nazaroff, Mr. Kevin B. Tannel and Ms. Naomi Olson while they were participants in an undergraduate research program coordinated by the Argonne Division of Educational Programs.

#### REFERENCES

- Bird, R. B., W. E. Stewart and E. N. Lightfoot, 1960: *Transport Phenomena*. Wiley, 780 pp.
- Bruno, R., 1978: A correction procedure for separating direct and diffuse insolation on a horizontal surface. *Solar Energy*, **20**, 97-100.
- Coulson, E. L., 1975: *Solar and Terrestrial Radiation*. Academic Press, 322 pp.
- Davies, J. A., 1979: Estimating the surface radiation balance and its components. *Modification of the Aerial Environment of Crops*, ASAE Monograph, 183-210.
- Drummond, A. J., 1956a: On the measurement of sky radiation. *Arch. Meteor. Geophys. Bioklim.*, **7**, 413-436.
- , 1956b: Notes on the measurement of natural illumination. *Arch. Meteor. Geophys. Bioklim.*, **7**, 437-465.
- Federer, C. A., and C. B. Tanner, 1966: Spectral distribution of light in the forest. *Ecology*, **47**, 555-560.
- Hoyt, D. V., 1977: Percent of possible sunshine and total cloud cover. *Mon. Wea. Rev.*, **105**, 648-652.
- Kerr, J. P., G. W. Thurtell and C. B. Tanner, 1967: An integrating pyranometer for climatological observer stations and meso-scale networks. *J. Appl. Meteor.*, **6**, 688-694.
- Liu, B. Y. H., and R. C. Jordan, 1960: The interrelationship and characteristic distribution of direct, diffuse and total solar radiation. *Solar Energy*, **4**, 1-19.
- Paltridge, G. W., and C. M. R. Platt, 1976: *Radiative Processes in Meteorology and Climatology*. Elsevier, 318 pp.
- Ruth, D. W., and R. E. Chant, 1976: The relationship of diffuse radiation to total radiation in Canada. *Solar Energy*, **18**, 153-154.
- Schultze, R. E., 1976: A physically based method of estimating solar radiation from sun cards. *Agric. Meteor.*, **16**, 85-101.
- Secrest, J. A., and I. Dirmhirn, 1979: Accuracies achievable with indirect measurements of the direct solar irradiance component. *Solar Energy*, **23**, 509-512.
- Shannon, J. D., M. L. Wesely and P. J. Brady, 1978: Objective sensor placement for sampling regional turbidity. *Atmos. Environ.*, **12**, 937-943.
- Stanhill, G., 1966: Diffuse sky and cloud radiation in Israel. *Solar Energy*, **10**, 96-101.
- Wesely, M. L., and R. C. Lipschutz, 1976a: An experimental study of the effects of aerosols on diffuse and direct solar radiation received during the summer near Chicago. *Atmos. Environ.*, **10**, 981-987.
- , and R. C. Lipschutz, 1976b: A method for estimating hourly averages of diffuse and direct solar radiation under a layer of scattered clouds. *Solar Energy*, **18**, 467-473.
- , W. W. Nazaroff and R. G. Everett, 1978: On the use of silicon photocells in the MAP3S turbidity network. Argonne National Laboratory Radiological and Environmental Research Division Annual Report, January-December 1977, ANL-77-65, Part IV, 118-124.